


EXPRESS LETTER

Open Access



Harmonic tremor from the deep part of Hakone volcano

Yohei Yukutake^{1*} , Ryou Honda², Motoo Ukawa³ and Kei Kurita⁴

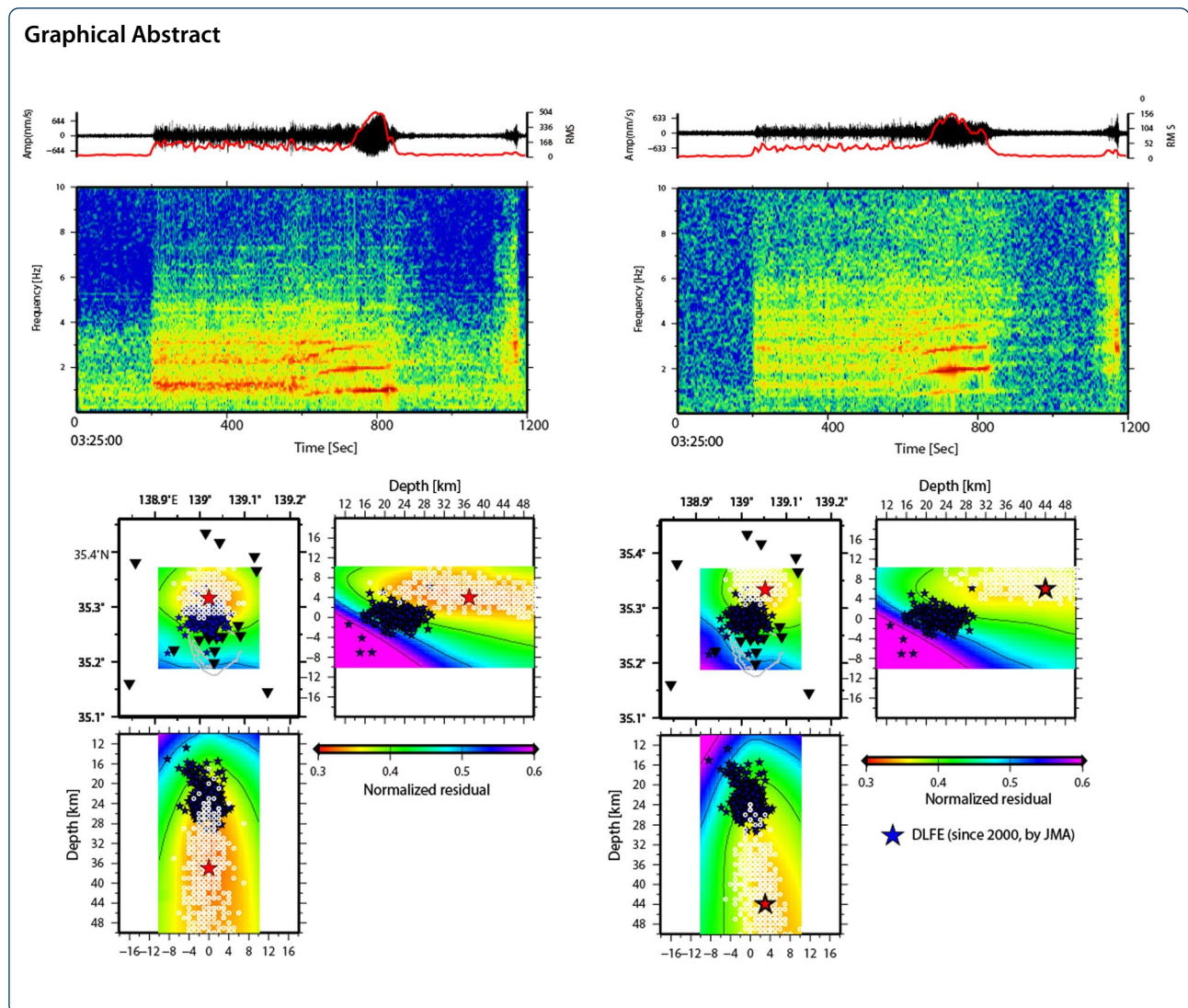
Abstract

The feeding system of magmatic fluid from the volcanic root to a shallow magma reservoir remains a poorly understood issue. Seismic events, including volcanic tremors and low-frequency earthquakes, in a deep part beneath volcanos are key observations for understanding the feeding system at the depth. Although deep low-frequency (DLF) earthquakes beneath volcanos have been recognized universally through dense seismic observations, volcanic tremors with harmonic frequency components originating at volcanic roots have rarely been observed. Here, we report the observation of a harmonic volcanic tremor event that occurred beneath the Hakone volcano on May 26, 2019. The tremor signal continued for approximately 10 min and was recognized at seismic stations 90 km away from the Hakone volcano. The apparent velocity of the tremor wave train is 5 km/s, corresponding to the S-wave velocity of the lower crust beneath the Hakone volcano. The frequency components varied with time. In the initial part of the tremor signal, a spectrum had a broad peak of around 1.2 Hz, whereas the tremor became harmonic with a sharp fundamental peak at 0.98 Hz in the latter part, increasing its amplitude. We estimated the source location of the volcanic tremor using the relative arrival times of the waveform envelope. The optimal source locations were estimated at a deep extension of the hypocenter distribution of the DLF earthquakes beneath the Hakone volcano, around the depth level of Moho discontinuity. The DLF earthquakes were activated immediately before the onset time of the volcanic tremor and continued for several months. The harmonic volcanic tremor may have been generated by the migration of magmatic fluid in the volcano's deep region.

Keywords: Harmonic tremor, Hakone volcano, Root of a volcano, Deep low-frequency earthquake

*Correspondence: yukutake@eri.u-tokyo.ac.jp

¹ Earthquake Research Institute, The University of Tokyo, 1-1-1 Yayoi, Bunkyo-ku, Tokyo, Japan
Full list of author information is available at the end of the article



Introduction

A volcanic tremor is defined as a continuous seismic signal observed near active volcanoes, lasting from several minutes to days. The seismic signal is observed before and during volcanic eruptions or sometimes independently. Although its driving mechanism is unclear, several physical models, involving the interactions of magmatic fluid, have been proposed (Chouet 1988; Julian 1994; Leet 1988; Rust et al. 2008; Takeo 2020). The location of a volcanic tremor is a key indicator to trace magmatic fluid (Ichihara and Matsumoto 2017) and at times reflects the eruption style (Battaglia et al. 2005). Volcanic tremor often shows harmonic characteristics in its spectrogram, with a fundamental frequency peak and its overtones. Numerous examples of harmonic tremors that occurred in shallow regions immediately below the vents of volcanoes have been reported in previous studies (e.g., Ichihara

et al. 2013; Kamo et al. 1977; Konstantinou and Schlindwein 2003; Maryanto et al. 2008; Ripepe et al. 2009).

Only few studies on volcanic tremors that occurred in the deep part of volcanoes have been reported in the literature. For example, Aki and Koyanagi (1981) reported a deep volcanic tremor originating around a 40-km depth beneath Kilauea, Hawaii. Ukawa and Ohtake (1987) also showed a continuous seismic signal characterized by a nearly monochromatic sinusoidal wave train radiated from a 30 km depth beneath Izu-Oshima 1 year before the 1986 eruption. The characteristics of observed waveforms reported in these studies are similar to those of volcanic tremors that occurred at shallow volcanoes, such as just beneath conduits (e.g., Takeo 2020). Ukawa and Ohtake (1987) interpreted that tremor signals were also induced by the movement of magmatic fluid in the deep part of volcanoes.

Around a deep part beneath volcanos, deep low-frequency (DLF) earthquakes that have low-frequency components compared to regular tectonic earthquakes with the same magnitude have also been observed. DLF earthquakes have been usually identified as isolated waveforms representing a P- or S-wave, although their onset is often unclear. Within the depth range of the middle crust to the upper mantle on Japanese Island, DLF earthquakes were recognized using a dense seismic observation network (Fig. 1a). DLF earthquakes beneath volcanos have also been detected in various regions (e.g., Nichols et al. 2011; Shapiro et al. 2017; Wech et al. 2020). Several studies have shown the physical model of DLF earthquakes related to the movement of magmatic fluid (Nakamichi et al. 2003) or the cooling of magma bodies (Aso and Tsai 2014; Wech et al. 2020). However, the generation mechanisms of DLF earthquakes, particularly mechanisms for seismic wave excitation with a long duration time, and their relation to deep volcanic tremors are unclear.

In the present study, we report a harmonic volcanic tremor that originated from a deep part beneath Hakone volcano, Central Japan, in the early morning of May 26, 2019. To the best of our knowledge, this constitutes the first report of a harmonic volcanic tremor that occurred in a deep region beneath a volcano, except for that in Hawaii reported by Aki and Koyanagi (1981), while there are numerous reports of shallow harmonic tremors in volcanos, as mentioned previously. This observation is essential for understanding the feeding process of magmatic fluid from volcanic roots. Here, we report the characteristics of the harmonic volcanic tremor as waveform records, spectrograms, and particle motion and estimate its source location. Moreover, we discuss the relationship between the deep harmonic tremor and DLF earthquakes in Hakone.

The Hakone volcano is a volcanic complex formed by several magma eruptions since 60 Ma (Nagai and Takahashi 2008) and a caldera volcano surrounded by the caldera rim with a diameter of approximately 10 km (Fig. 1b). Remarkable earthquake swarms have often been observed within a shallower depth of 7 km (Fig. 1b, c), accompanied by a crustal expansion detected by a Global Navigation Satellite System (Harada et al. 2018). Active fumarolic activity persists in Owakudani on the north flank of the central cone, where a small phreatic eruption occurred at the end of June 2015 (Mannen et al. 2018). DLF earthquakes have also occurred within the depth range of 20–30 km (Fig. 1c). The DLF earthquakes were activated before volcanic activities, such as earthquake swarms, crust expansion due to the inflation of pressure source around the depth of 7 km, and phreatic eruption (Yukutake et al. 2019), suggesting that the

activation of DLF earthquakes reflects the increment of the supply of magmatic fluid at the depth. The locations of shallow magma reservoir and dehydrated hydrothermal fluid were estimated to be 9 and 6 km, respectively, using the seismic tomography method (Yukutake et al. 2015, 2021).

Characteristics of volcanic tremor

Figure 2 shows the record section of vertical velocity waveforms observed at the seismic stations installed by the Hot Springs Research Institute of Kanagawa Prefecture and the National Research Institute for Earth Science and Disaster Resilience Hi-net (NIED 2019) within 100 km (Fig. 2d) from the Hakone volcano during 03:00–04:00 on May 26, 2019 (JST = UT + 9 h). The main tremor started at around 3:28 (1680 s in Fig. 2a–c) and lasted 10 min, increasing in amplitude at its later part. The tremor signal was initially observed at the N.ASGH Hi-net station (Fig. 1a) located at the northern part of the Hakone volcano and recognized at the stations approximately 90 km away from Hakone, propagating at an apparent velocity of 5 km/s. Another tremor signal with a duration of 2 min can also be seen at around 3:03 (180 s in Fig. 2a, b).

Figure 3 shows the spectra of the volcanic tremor starting from 03:28 at the stations near the Hakone volcano. The early part of the tremor, 200–600 s in Fig. 3, shows a broad spectral peak around 1.2 Hz (Fig. 3e). The peak at 1.2 Hz in the spectrum was observed at multiple stations; however, the spectral characteristics at a higher frequency differed at each station. The results suggest that the peak at 1.2 Hz reflected the source effect. Meanwhile, the spectrum component at a higher frequency was affected by the path effect from source to station. The amplitude of the tremor gradually increased after 600 s and became a maximum of around 700 s. After the peak of the root mean square (RMS) amplitude, the tremor signal decayed abruptly. As the tremor amplitude increases after 600 s, the frequency component of the tremor changes to a harmonic with a fundamental mode at approximately 0.98 Hz, showing several spectral peaks corresponding to the overtone modes (Fig. 3f). These peaks in the spectra and overtone modes were observed at several stations; thus, the harmonic feature of a spectrum was influenced by the source effect. We also observed the gliding of peaks during the initial part of the harmonic tremor (600–760 s), during which the frequency of the fundamental peak changed from 0.90 to 0.98 Hz. The particle motion of each station in the horizontal plane during the early part of the tremor is unstable and varies in time. In the latter part, when its amplitude increases, the trajectory is stable, which

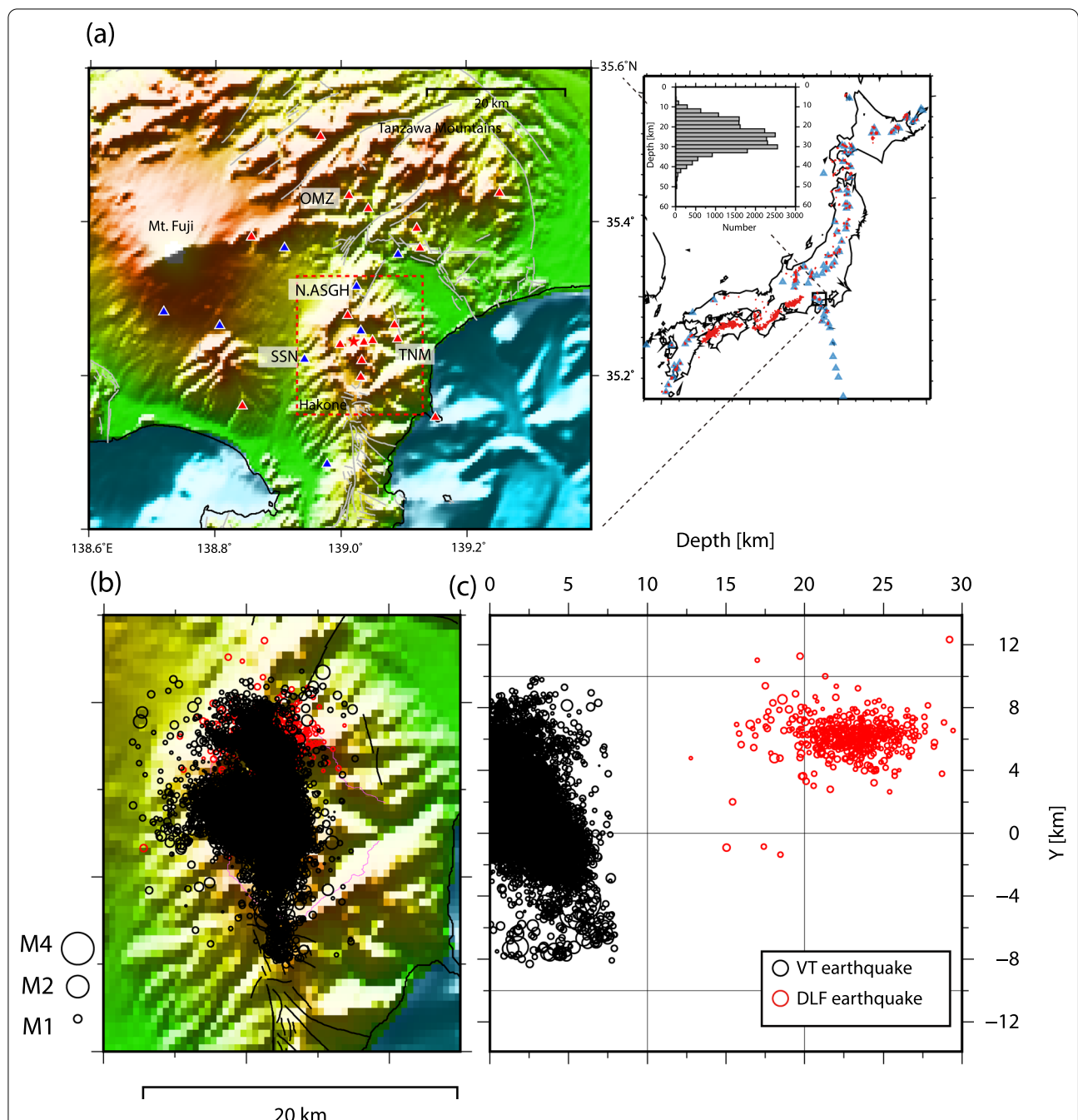


Fig. 1 Map of the Hakone volcano. **a** Relief map of the Hakone volcano and its vicinity. Triangles show the locations of seismic stations. The seismic data at the red triangle stations were used to analyze the envelope correlation. Spectrograms recorded at OMZ, N.ASGH, SSN, and TNM stations are shown in Fig. 3. The red star shows the location of Owakudani. The red broken rectangle corresponds to the region showing in **b**. The right figure denotes the target area for the Japanese islands, indicating the deep low-frequency (DLF) earthquake epicenters (red) determined by the Japan Meteorological Agency (JMA) and active volcanos (blue triangles). The distribution of banded hypocenters in southwest Japan corresponds to non-volcanic low-frequency earthquakes that occur at the boundary of the subducting Philippine Sea Slab (Katsumata and Kamaya 2003). The depth–frequency distribution of DLF earthquakes excepted for the non-volcanic event along to the Philippine Sea Slab is also showing. **b** Seismic activity beneath the Hakone volcano during the past two decades and **c** projected on the N–S depth section. The open black circles show the hypocenters of volcano tectonic (VT) earthquakes determined by the Hot Springs Research Institute (HSRI). The red circles represent the hypocenter of DLF earthquakes by JMA. The size of each circle corresponds to the local magnitude of the earthquake

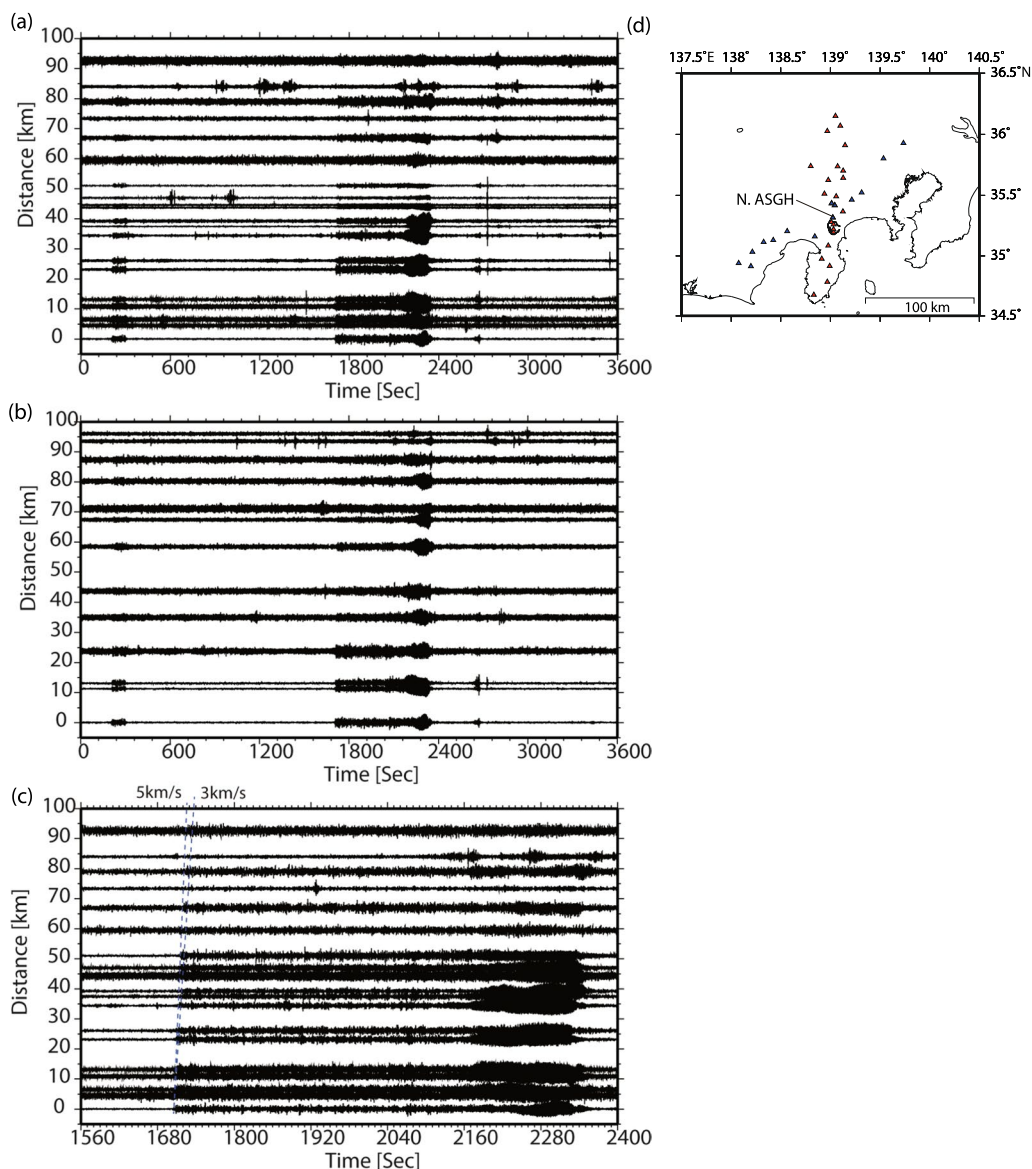


Fig. 2 Record section of velocity waveforms recorded at HSRI and Hi-net stations within 100 km from N.ASGH station during 03:00–04:00 on May 26, 2019 (JST = UT + 9 h). **a** and **b** show the record sections along to N–S (red triangles in **d**) and WSW–ENE (blue triangles in **d**) sections, respectively. **c** A magnified plot of **a** during the main tremor signal between 1560 and 2400 s. The two blue broken lines correspond to the traces with the apparent velocity of 3 and 5 km/s. The amplitude of each station was normalized. **d** Station distribution

seems to be mainly oriented to the radial directions toward the N.ASGH station (Additional file 1: Figure S1 and Additional file 2: Movie S1). The particle motions in the radial–vertical plane toward the N.ASGH station are shown in Additional file 1: Figure S2. The particle motions at multiple stations were not consistent with the Rayleigh wave trajectory. The trajectories were also oriented predominantly to the horizontal direction.

Estimation of source location

We estimated the source location of the volcanic tremor using the relative arrival times of waveform envelopes across the stations. The spatial distribution of seismic amplitudes has often been used to estimate the source location of tremors (Battaglia and Aki 2003; Kumagai et al. 2010). For the Hakone volcano, a highly resolved three-dimensional (3-D) velocity structure was obtained

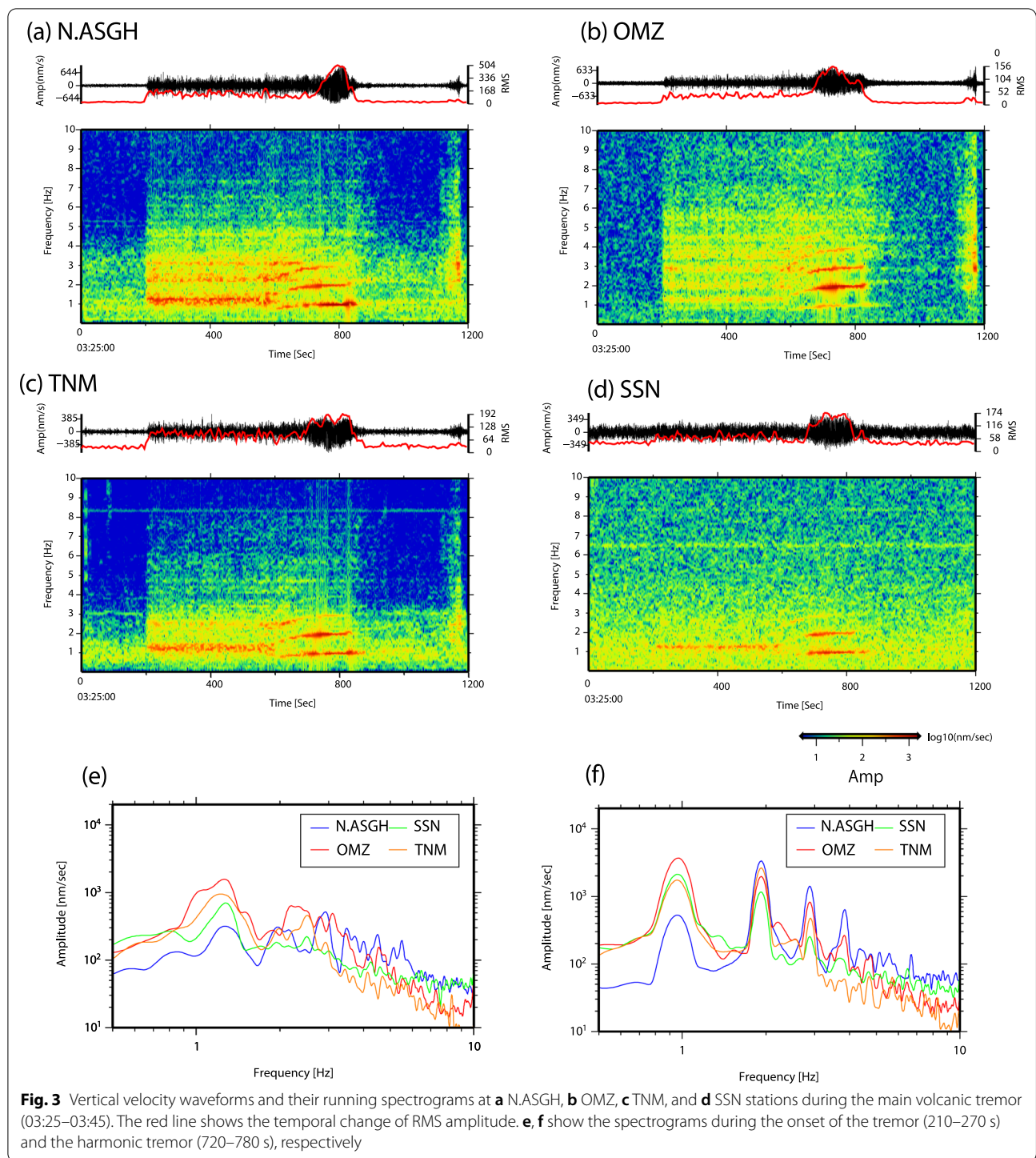


Fig. 3 Vertical velocity waveforms and their running spectrograms at **a** N.ASGH, **b** OMZ, **c** TNM, and **d** SSN stations during the main volcanic tremor (03:25–03:45). The red line shows the temporal change of RMS amplitude. **e, f** show the spectrograms during the onset of the tremor (210–270 s) and the harmonic tremor (720–780 s), respectively

using the tomography method (Yukutake et al. 2015), which enables the estimation of the travel time difference between each station pair precisely, resulting in the reliable estimation of the tremor source location. We obtained the differential arrival times of the coherent phases by the cross-correlation of waveform envelopes, following a

procedure developed by Obara (2002). Some studies have successfully determined the location of tremor sources in the volcanic region using the differential arrival times (Uchida 2014; Yukutake et al. 2017).

In this study, we used the velocity waveform record from 17 stations with high signal-to-noise ratios located

in and around the Hakone volcano (Fig. 1). The natural frequencies of the seismometers at these stations were 1 Hz. The sampling frequency is 200 Hz for the stations of HSRI and 100 Hz for the other stations. We calculated the RMS envelope using the three-component waveform within a 1-min time window after the frequency response of a seismometer was removed. We applied a band-pass filter between 0.5 and 5.0 Hz, given the frequency components of the tremor, and a 2-s sliding time window to obtain the RMS amplitude at each station. The cross-correlation coefficients of 1-min envelope traces across all station pairs were obtained by moving the traces with every sampling interval. The lag time with the maximum correlation coefficient was used as the differential arrival time. We only used differential arrival times that had a correlation coefficient ≥ 0.8 .

When we obtained the differential arrival times meeting the condition of the cross-correlation for at least 100 station pairs, we estimated the tremor source location. This threshold for the station pairs was met only by the

time windows during the onsets of the tremor starting at 3:03 and 3:28. We performed a grid search at intervals of 2 km, setting the nodes of grids within ± 20 km in the E–W and N–S directions and from 0 to 100 km in the vertical direction, centered at the N.ASGH station. We calculated the synthetic arrival times from each grid node to the stations using the three-dimensional velocity structure of the Hakone volcano by Yukutake et al. (2015), assuming that the seismic waves represented by the envelopes propagated at S-wave velocities. The tremor onset propagated with an apparent velocity of 5 km/s (Fig. 2c), which agrees with the S-wave velocity in the lower crust beneath the Hakone volcano (Yukutake et al. 2021). The particle motions on the radial–vertical plane (Additional file 1: Figure S2), in which oscillations along the horizontal direction is dominant, also suggest that the wave train of the volcanic tremors primarily comprise the S wave. We calculated the residuals as the sum of misfit between the observed and synthetic differential arrival times for all station pairs and searched for

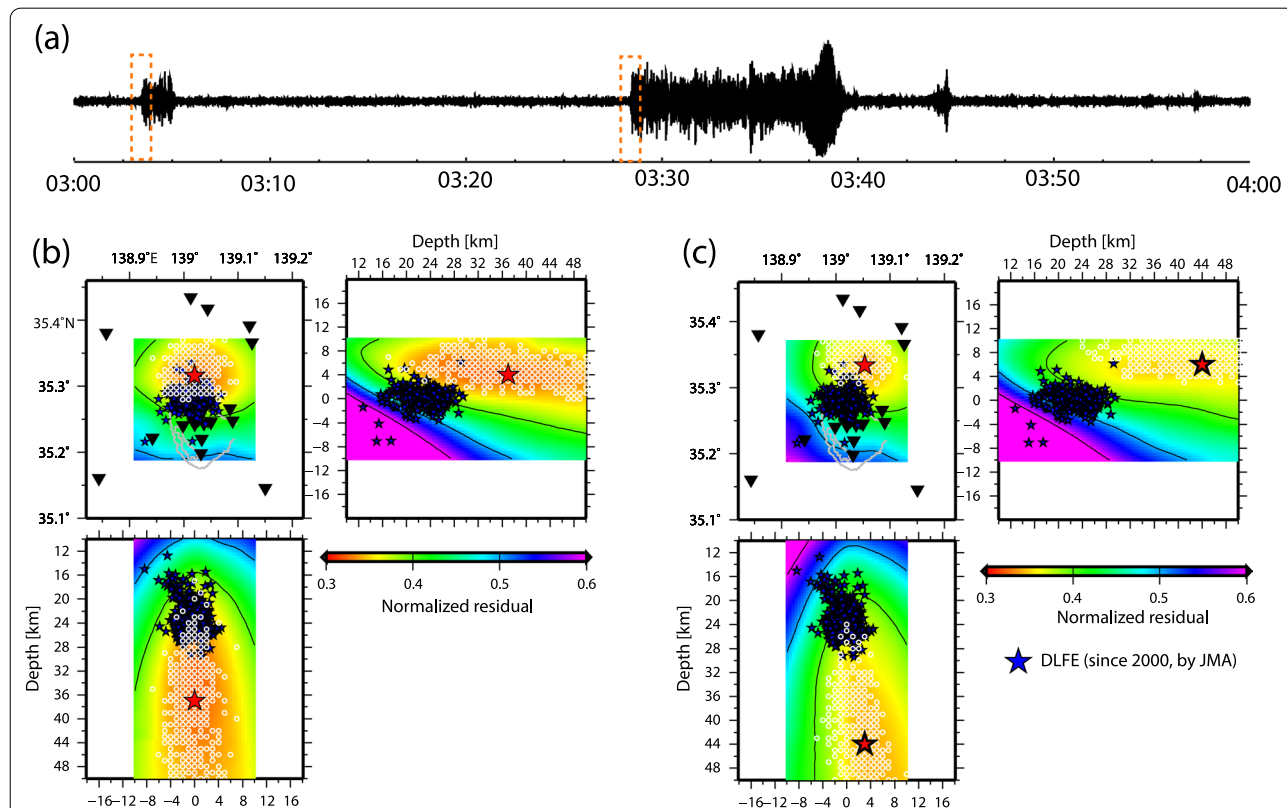


Fig. 4 Results of the envelope correlation method. **a** Velocity vertical waveform at the N.ASGH station during 03:00–04:00 May 26, 2019. The orange broken rectangles indicate the 1-min time window used for the envelope correlation analysis. **b** and **c** show the results of source estimation for the earlier and later time windows in **a**. The red stars in **b** and **c** show the best locations of volcanic tremors for each time window. The color contours represent the normalized residual projected on the horizontal plane at a depth of 37 km, N–S, and E–W sections. The white circles show the result of the bootstrap resampling method. The blue stars indicate the hypocenters of DLF earthquakes based on the JMA unified hypocenter catalog

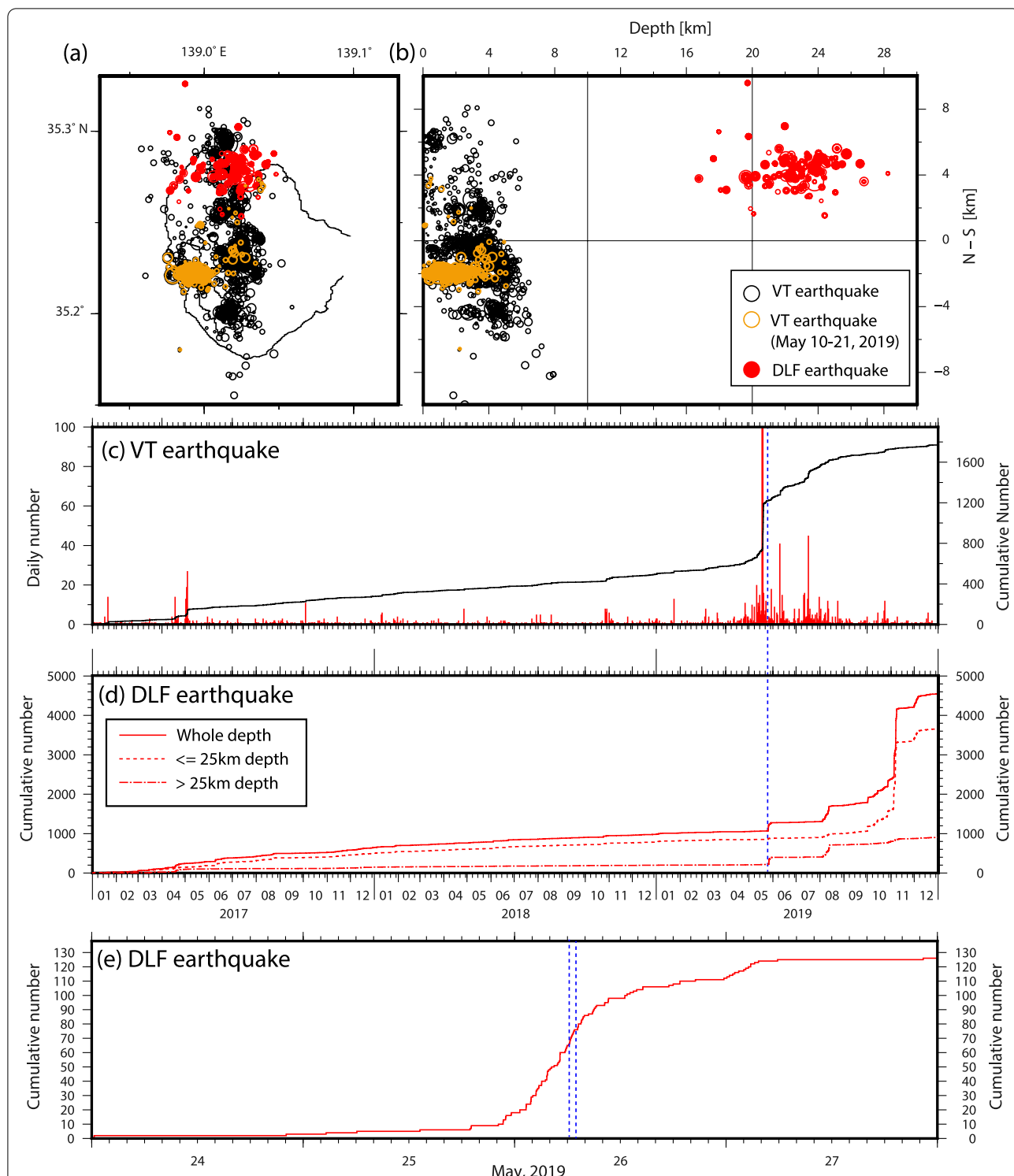


Fig. 5 Seismic activity beneath the Hakone volcano before and after the volcanic tremor. **a** Epicentral distribution of volcanic tremor and DLF earthquakes and **b** their depth distribution along with the N-S section. The black (or orange) open and red solid circles show the hypocenters of VT and DLF earthquakes, respectively. The orange circles denote the hypocenters of the earthquake swarm that occurred in May 2019. **c** The cumulative and the daily number of VT earthquakes, and **d** the cumulative number of DLF earthquakes. The two broken lines in **d** show the cumulative curves of DLF earthquakes at shallower and deeper depths than 25 km. **e** A magnified plot of the cumulative curve of DLF earthquakes during May 24–27, 2019. The vertical blue broken lines indicate the occurrence times of the volcanic tremors. The DLF earthquakes were detected by a matched filter method, whereas the VT earthquakes are based on the hypocenter catalog obtained by HSRI routine analysis

the optimal tremor source location that minimized the residual. We applied a bootstrap resampling method 500 times to assess the tremor location uncertainties.

Figure 4 shows the results of tremor source estimation for the waveform records of two tremor onsets. The optimal solutions for the two time windows were determined at the depths of 37 and 45 km in the northern part of the Hakone caldera. These locations correspond to the deep extension of the region where the DLF earthquakes have occurred in the past two decades. On the other hand, the hypocenter of DLF earthquakes by Japan Meteorological Agency (JMA) were determined by the 1-D velocity structure model. Meanwhile, we estimated the source locations of the volcanic tremors using the 3-D velocity structure. Yukutake et al. (2021) determined the hypocenters of DLF earthquakes using the 3-D velocity structure and showed that DLF earthquakes distribute within the depth range of 17–25 km. Therefore, the difference in velocity structures does not affect the discussion on the source depth between DLF earthquakes and volcanic tremors.

Discussion

The optimal tremor source locations were determined at deep extensions of the DLF earthquake distribution (Fig. 4). According to the bootstrap results, the uncertainty of hypocenter location in the vertical direction is more than that in the horizontal direction because we estimated the tremor location considering the only differential time of S wave. However, the source regions of the two seismic activities are separated, given the confidence region of tremor locations defined by the distribution of solutions due to the bootstrap resampling. The volcanic tremors likely occurred in the deep extensions of the DLF earthquake distribution. We also show the record section along the same N–S section in Fig. 2a and c for the tectonic earthquake that occurred 10 km NNE from the epicenters of the volcanic tremors and at a 28 km depth (Additional file 1: Figure S3), respectively. The apparent velocity of S-wave onsets was ~ 5 km/s, which is consistent with the propagation of tremor onsets (Fig. 2c) and the S-wave velocities in the lower crust (Matsubara et al. 2008). When we estimated the location of the tremor source using the three-dimensional P wave velocity structure by Yukutake et al. (2015), the optimal source depths for the two time windows were 16 and 25 km (Additional file 1: Figure S4). However, the rms residuals for the travel time difference using the P wave velocity structure were larger compared with the S-wave velocity. The residual values using the P wave velocity were 1.308 and 1.441 s for the two time windows. The values were 1.265 and 1.409 s using the S-wave velocity. The particle motions in the radial–vertical plane (Additional file 1:

Figure S2) suggested a dominant oscillation that was oriented to the horizontal direction at multiple stations. These results agree with our estimations that the tremor signals radiated from the deep part beneath the Hakone volcano, and propagated with the S-wave velocity. Ishise et al. (2021) estimated that the depth of Moho discontinuity beneath the Hakone volcano is approximately 40 km using the anisotropic tomography method. These results suggest that the tremor signal radiated around the depth level of the uppermost mantle or lower crust. The harmonic tremor in this depth region beneath the volcano is quite rare. Aki and Koyanagi (1981) reported the deep volcanic tremor radiated from a depth around 40 km beneath Kilauea. Although the tectonic setting between two regions is different; Kilauea volcano is a hot spot volcano, while the Hakone volcano is an island arc volcano; the volcanic tremor reported herein is one of the deepest cases ever reported globally.

The duration time of the tremor is approximately 10 min; the frequency components change with time. In the latter part of the signal, the tremor became harmonic, increasing its amplitude. The harmonic features of the volcanic tremor were observed at several stations around the tremor epicenter (Fig. 3f). Therefore, the frequency components reflect not the path or site effect but the source process. One model that explains a harmonic tremor is the resonance of fluid-filled crack (Chouet 1988; Kumagai et al. 2002). If we consider the resonance model, the gliding of the frequency component in the later part of the tremor signal might reflect the temporal variation of the resonator size such as a magmatic fluid reservoir or the sound velocity of the fluid within the resonator. For example, Maeda and Kumagai (2013) showed an analytical solution for longitudinal resonance frequencies of a fluid-filled crack. Based on the theoretical model, the gliding of the frequency from 0.90 to 0.98 Hz at the fundamental mode during the initial part of the harmonic tremor (Fig. 3) can be explained by considering the length change of the crack with 0.5 m aperture from 265 to 250 m, assuming basaltic magma with bulk modulus and fluid density of 18 GPa and 2650 kg/m³, respectively (Schubert 2015). Using numerical waveform modeling, Haruyama et al. (2020) demonstrated that successive impulsive pressure transients must act on the resonator to generate the harmonic seismic signal within a long duration. They also showed that a remarkable harmonic signal with increasing its amplitude generates, when the time interval of impulsive pressure is close to a two-way travel time in the resonator. The increase in tremor amplitude in the later part of the signal might reflect the temporal change of the time interval of impulsive pressure. However, a physical mechanism for this successive impulsive pressure has not been well-modeled.

Another model for a volcanic tremor is a self-excited oscillation induced by fluid flow within an elastic channel (Julian 1994). Ozaki et al. (2022) successfully modeled the tremor signal presented in this study, including the frequency components and duration, by modifying Julian's model to oscillations in an elliptical channel, assuming elastic parameters at the depth level of the lower crust.

To discuss the relationship between the volcanic tremor and DLF earthquakes beneath the Hakone volcano, we investigated the activity of the DLF earthquakes before and after the tremor signal. We used a seismic catalog of the DLF earthquakes detected by a matched filter method, following the procedure in Yukutake et al. (2019). In the matched filter method, the DLF earthquakes during the past two decades listed in the JMA unified seismic catalog were used as template events. The activation of the DLF earthquakes started immediately before the onset of the tremor and continued after the occurrence of the tremor (Fig. 5d, e). The DLF earthquakes had been quiescent for two years before May 25, 2019 (Fig. 5d) and become active just before this volcanic tremor. The seismic rate of the DLF earthquakes maintained a high level for several months, showing bust-like increases several times (Fig. 5d). During the initial term of the activity (May–August 2019), the DLF earthquake mainly occurred in the region deeper than 25 km (Fig. 5d). On the other hand, the centroid of the DLF earthquake distribution shifted to the shallow part (≤ 25 -km depth) during the latter term (October–November 2019), indicating the migration of the hypocenter region from the deep to shallow part. The activation of the DLF earthquakes beneath the Hakone volcano is interpreted to reflect an increase in the feeding rate of magmatic fluid at this depth (Yukutake et al. 2019). The intrusion of magmatic fluid from the depth around the Moho discontinuity likely triggers the DLF earthquakes and the volcanic tremor. Notably, the DLF earthquakes activated several hours before the onset of the volcanic tremor (Fig. 5e). This result suggests that the fluid supply started at the timing of the DLF earthquake activation before the volcanic tremor. The harmonic tremor signal may be generated when several factors such as velocity, density, or viscosity of fluid match the condition to cause a nonlinear oscillation of the channel (Julian 1994). The difference in the source depth between the DLF earthquakes and volcanic tremor might reflect differences in the properties of magmatic fluid, geometry of fluid path, and rheology of surrounding host rock. No DLF earthquake could be detected during the wave trains of the volcanic tremors by the matched filter method, suggesting that the radiation pattern or location of the tremor differs from those of the DLF earthquakes.

The earthquake swarm in the shallow part of the Hakone volcano was observed 2 weeks before the tremor and at the activation of the DLF earthquakes and volcanic tremor (Fig. 5c). Yukutake et al. (2019) indicated that most past swarm activities occurred after the DLF earthquake activation. The reason the earthquake swarm in 2019 occurred before the DLF activation is unclear. Because the swarm activity occurred on the western part of Hakone caldera (orange circles in Fig. 5a, b), the seismicity in this area might not be linked to the activity in the deep part of the volcano.

Conclusion

In this study, we show the harmonic volcanic tremor observed at the seismic stations near the Hakone volcano on May 26, 2019. The main part of the tremor signal continued for approximately 10 min. The frequency components change with time. In the latter part of the signal, the tremor became a harmonic, increasing its amplitude. The source locations of the volcanic tremors were estimated at deep extensions of the DLF earthquake distribution, around the depth level of Moho discontinuity beneath the Hakone volcano. The DLF earthquakes activated immediately before the onset of the volcanic tremor and continued for several months. This volcanic tremor likely occurred in relation to the DLF earthquake activation. The harmonic volcanic tremor may be generated by the migration of magmatic fluid in the deep region of the volcano. Quantitative physical modeling for the volcanic tremor is a future research direction and will provide relevant information to obtain the mechanism of magma movement at volcano roots.

Abbreviations

DLF earthquake: Deep low-frequency earthquakes; JMA: Japan Meteorological Agency; VT: Volcano tectonic earthquakes.

Supplementary Information

The online version contains supplementary material available at <https://doi.org/10.1186/s40623-022-01700-8>.

Additional file 1: Figure S1. Particle motions on the horizontal plane during the main volcanic tremor (03:25–03:45). (a) The vertical waveform at the N.ASGH stations. Red trajectories in (b) and (c) show the particle motions of velocity waveform on the horizontal plane at each station during the period of harmonic tremor as indicated by the red and yellow rectangles in (a), respectively. **Figure S2.** Particle motions on the radial–vertical plane during the main volcanic tremor (03:25–03:45). (a) The vertical waveform at N.ASGH stations. Red trajectories in (b) and (c) show particle motions of the velocity waveform on the radial–vertical plane at each station during the period of harmonic tremor during the periods indicated by the red and yellow rectangles in (a), respectively. The radial direction of each trajectory is eastward as shown in the inset of (c). Note that the particle motion in N.ASGH on the radial–vertical plane is not shown owing to the differences in the natural frequency of the horizontal and vertical seismometers. **Figure S3.** Record section of the tectonic earthquake (35.44010°N, 139.10108°E, depth = 28.46 km, local magnitude

= 2.5) that occurred 10 km horizontally NNE from the epicenter of the volcanic tremor. (a) Record section 100 km from N.ASGH station along to N–S section. Zero second on the time axis corresponds to the origin time (09/06/2015 12:52:25 JST). (b) Station distribution. The stations used in this record section are the same as that shown in Figures 2a and 2c. The yellow star shows the epicenter of the tectonic earthquake. **Figure S4.** Results of the envelope correlation method assuming the P wave velocity structure. The meaning of (a)–(c) is the same as in Figure 4 in the main text.

Additional file 2: Movie S1. Animation to show the temporal change of the particle motions on the horizontal plane.

Acknowledgements

We used the waveform record at the seismic station installed by the Hot Springs Research Institute of Kanagawa Prefecture, National Research Institute for Earth Science and Disaster Resilience Hi-net, and Japan Meteorological Agency (JMA). We thank Dr. Takuto Maeda and Dr. Masahiro Kosuga for helpful discussion. We also thanks Dr Haruhisa Nakamichi and Dr. Kostas Konstantinou and the anonymous reviewer for helpful comments.

Author contributions

YY analyzed the data and wrote the manuscript. RH carried out seismic observations. KK and MU supported the data processing and assisted with the interpretation. All authors read and approved the final manuscript.

Funding

The present study was supported by JSPS KAKENHI Grant No. 22K0375.

Availability of data and materials

The waveform data presented in this study can be obtained from the web page of National Research Institute for Earth Science and Disaster Resilience Hi-net (<https://www.hinet.bosai.go.jp>).

Declarations

Ethics approval and consent to participate

Not applicable.

Consent for publication

Not applicable.

Competing interests

The authors declare that they have no competing interests.

Author details

¹Earthquake Research Institute, The University of Tokyo, 1-1-1 Yayoi, Bunkyo-ku, Tokyo, Japan. ²Hot Springs Research Institute of Kanagawa Prefecture, Iriuda 586, Odawara, Kanagawa, Japan. ³Department of Earth and Environmental Sciences, College of Humanities and Sciences, Nihon University, 3-25-40 Sakurajosui, Setagaya-ku, Tokyo, Japan. ⁴The Earth-Life Science Institute of Tokyo Institute of Technology, 2 Chome-12-1 Ookayama, Meguro City, Tokyo, Japan.

Received: 14 June 2022 Accepted: 29 August 2022

Published online: 21 September 2022

References

- Aki K, Koyanagi R (1981) Deep volcanic tremor and magma ascent mechanism under Kilauea Hawaii. *J Geophys Res* 86:7095–7109. <https://doi.org/10.1029/JB086iB08p07095>
- Aso N, Tsai VC (2014) Cooling magma model for deep volcanic long-period earthquakes. *J Geophys Res* 119:8442–8456. <https://doi.org/10.1002/2014JB011180>
- Battaglia J, Aki K (2003) Location of seismic events and eruptive fissures on the Piton de la Fournaise volcano using seismic amplitudes. *J Geophys Res.* <https://doi.org/10.1029/2002JB002193>
- Battaglia J, Aki K, Ferrazzini V (2005) Location of tremor sources and estimation of lava output using tremor source amplitude on the Piton de la Fournaise volcano: 1. Location of tremor sources. *J Volcanol Geotherm Res* 147:268–290. <https://doi.org/10.1016/j.jvolgeores.2005.04.005>
- Chouet B (1988) Resonance of a fluid-driven crack: radiation properties and implications for the source of long-period events and harmonic tremor. *J Geophys Res* 93:4375–4400. <https://doi.org/10.1029/JB093iB05p04375>
- Harada M, Doke R, Mannen K, Itadera K, Satomura M (2018) Temporal changes in inflation sources during the 2015 unrest and eruption of Hakone volcano. *Jpn Earth Planets Space* 70:152. <https://doi.org/10.1186/s40623-018-0923-4>
- Haruyama T, Kosuga M, Maeda T (2020) Characteristic of seismic waveforms of deep low-frequency earthquakes beneath volcanoes: generation mechanism based on numerical modeling. *Tohoku J Nat Disaster Sci* 56:135–140 (in Japanese)
- Ichihara M, Matsumoto S (2017) Relative source locations of continuous tremor before and after the subplinian events at Shinmoe-dake, in 2011. *Geophys Res Lett.* <https://doi.org/10.1002/2017gl075293>
- Ichihara M, Lyons JJ, Yokoo A (2013) Switching from seismic to seismo-acoustic harmonic tremor at a transition of eruptive activity during the Shinmoe-dake 2011 eruption. *Earth Planets Space* 65:633–643. <https://doi.org/10.5047/eps.2013.05.003>
- Ishise M, Kato A, Si S, Nakagawa S, Hirata N (2021) Improved 3-D P wave azimuthal anisotropy structure beneath the Tokyo metropolitan area, Japan: new interpretations of the dual subduction system revealed by seismic anisotropy. *J Geophys Res.* <https://doi.org/10.1029/2020JB021194>
- Julian BR (1994) Volcanic tremor: nonlinear excitation by fluid flow. *J Geophys Res* 99:11859–11877. <https://doi.org/10.1029/93JB03129>
- Kamo K, Furuzawa T, Akamatsu J (1977) Some natures of volcanic micro-tremors at the Sakura-Jima volcano. *Bull Volcanol Soc Jpn* 22:41–58 (in Japanese with English Abstract)
- Katsumata A, Kamaya N (2003) Low-frequency continuous tremor around the Moho discontinuity away from volcanoes in the southwest Japan. *Geophys Res Lett* 30:20-21-20–24. <https://doi.org/10.1029/2002GL015981>
- Konstantinou KI, Schlindwein V (2003) Nature, wavefield properties and source mechanism of volcanic tremor: a review. *J Volcanol Geotherm Res* 119:161–187. [https://doi.org/10.1016/S0377-0273\(02\)00311-6](https://doi.org/10.1016/S0377-0273(02)00311-6)
- Kumagai H, Chouet BA, Nakano M (2002) Temporal evolution of a hydrothermal system in Kusatsu-Shirane volcano, Japan, inferred from the complex frequencies of long-period events. *J Geophys Res* 107:ESE.9-1-ESE.9-10. <https://doi.org/10.1029/2001JB000653>
- Kumagai H et al (2010) Broadband seismic monitoring of active volcanoes using deterministic and stochastic approaches. *J Geophys Res.* <https://doi.org/10.1029/2009JB006889>
- Leet RC (1988) Saturated and subcooled hydrothermal boiling in groundwater flow channels as a source of harmonic tremor. *J Geophys Res* 93:4835–4849. <https://doi.org/10.1029/JB093iB05p04835>
- Maeda Y, Kumagai H (2013) An analytical formula for the longitudinal resonance frequencies of a fluid-filled crack. *Geophys Res Lett* 40:5108–5112. <https://doi.org/10.1002/grl.51002>
- Mannen K, Yukutake Y, Kikugawa G, Harada M, Itadera K, Takenaka J (2018) Chronology of the 2015 eruption of Hakone volcano, Japan: geological background, mechanism of volcanic unrest and disaster mitigation measures during the crisis. *Earth Planets Space* 70:68. <https://doi.org/10.1186/s40623-018-0844-2>
- Maryanto S, Iguchi M, Tameguri T (2008) Constraints on the source mechanism of harmonic tremors based on seismological, ground deformation, and visual observations at Sakurajima volcano, Japan. *J Volcanol Geotherm Res* 170:198–217. <https://doi.org/10.1016/j.jvolgeores.2007.10.004>
- Matsubara M, Obara K, Kasahara K (2008) Three-dimensional P- and S-wave velocity structures beneath the Japan islands obtained by high-density seismic stations by seismic tomography. *Tectonophysics* 454:86–103. <https://doi.org/10.1016/j.tecto.2008.04.016>
- Nagai M, Takahashi M (2008) Geology and eruptive history of Hakone volcano, Central Japan. *Res Rep Kanagawa Prefect Mus Nat Hist* 13:25–42 (in Japanese with English Abstract)
- Nakamichi H, Hamaguchi H, Tanaka S, Ueki S, Nishimura T, Hasegawa A (2003) Source mechanisms of deep and intermediate-depth low-frequency earthquakes beneath Iwate volcano, northeastern Japan. *Geophys J Int* 154:811–828. <https://doi.org/10.1046/j.1365-246X.2003.01991.x>
- Nichols ML, Malone SD, Moran SC, Thelen WA, Vidale JE (2011) Deep long-period earthquakes beneath Washington and Oregon volcanoes. *J*

- Volcanol Geotherm Res 200:116–128. <https://doi.org/10.1016/j.jvolgeores.2010.12.005>
- NIED (2019) NIED Hi-net, National Research Institute for Earth Science and Disaster Resilience. <https://doi.org/10.17598/NIED.0003>
- Obara K (2002) Nonvolcanic deep tremor associated with subduction in Southwest Japan. *Science* 296:1679–1681. <https://doi.org/10.1126/science.1070378>
- Ozaki T, Yukuake Y, Ichihara M (2022) Modeling of harmonic volcanic tremor occurred in the deep part of Hakone volcano, Central Japan. Abstract of Japan Geoscience Union Meeting 2022:SCG54-P03
- Ripepe M, Delle Donne D, Lacanna G, Marchetti E, Olivieri G (2009) The onset of the 2007 Stromboli effusive eruption recorded by an integrated geophysical network. *J Volcanol Geotherm Res* 182:131–136. <https://doi.org/10.1016/j.jvolgeores.2009.02.011>
- Rust AC, Balmforth NJ, Mandre S (2008) The feasibility of generating low-frequency volcano seismicity by flow through a deformable channel. *Geol Soc Lond Special Publ* 307:45–56. <https://doi.org/10.1144/sp307.4>
- Schubert G (2015) *Treatise on geophysics*, vol 2nd. Elsevier, Amsterdam. <https://doi.org/10.1016/C2009-1-28330-4>
- Shapiro NM, Droznin DV, Droznina SY, Senyukov SL, Gusev AA, Gordeev EI (2017) Deep and shallow long-period volcanic seismicity linked by fluid-pressure transfer. *Nat Geosci* 10:442. <https://doi.org/10.1038/ngeo2952>
- Takeo M (2020) Harmonic tremor model during the 2011 Shinmoe-dake eruption, Japan. *Geophys J Int* 224:2100–2120. <https://doi.org/10.1093/gji/ggaa477>
- Uchida H (2014) Hypocenter distribution and source mechanism of B-type earthquakes at Miyakejima volcano. Doctoral Thesis, Tohoku University
- Ukawa M, Ohtake M (1987) A monochromatic earthquake suggesting deep-seated magmatic activity beneath the Izu-Ooshima volcano, Japan. *J Geophys Res* 92:12649–12663. <https://doi.org/10.1029/JB092iB12p12649>
- Wech AG, Thelen WA, Thomas AM (2020) Deep long-period earthquakes generated by second boiling beneath Mauna Kea volcano. *Science* 368:775–779. <https://doi.org/10.1126/science.aba4798>
- Yukutake Y, Honda R, Harada M, Arai R, Matsubara M (2015) A magma-hydrothermal system beneath Hakone volcano, Central Japan, revealed by highly resolved velocity structures. *J Geophys Res* 120:3293–3308. <https://doi.org/10.1002/2014jb011856>
- Yukutake Y et al (2017) Analyzing the continuous volcanic tremors detected during the 2015 phreatic eruption of the Hakone volcano. *Earth Planets Space* 69:164. <https://doi.org/10.1186/s40623-017-0751-y>
- Yukutake Y, Abe Y, Doke R (2019) Deep low-frequency earthquakes beneath the Hakone volcano, Central Japan, and their relation to volcanic activity. *Geophys Res Lett*. <https://doi.org/10.1029/2019gl084357>
- Yukutake Y, Abe Y, Honda R, Sakai S (2021) Magma reservoir and magmatic feeding system beneath Hakone volcano, Central Japan, revealed by highly resolved velocity structure. *J Geophys Res*. <https://doi.org/10.1029/2020JB021236>

Publisher's Note

Springer Nature remains neutral with regard to jurisdictional claims in published maps and institutional affiliations.

Submit your manuscript to a SpringerOpen® journal and benefit from:

- Convenient online submission
- Rigorous peer review
- Open access: articles freely available online
- High visibility within the field
- Retaining the copyright to your article

Submit your next manuscript at ► [springeropen.com](https://www.springeropen.com)
